Candidates for three-quasiparticle K isomers in odd-even Md–Rg nuclei

P. Jachimowicz,[1] M. Kowal,[2,*] and J. Skalski[2]
[1]*Institute of Physics, University of Zielona Góra, Z. Szafrana 4a, 65-516 Zielona Góra, Poland*
[2]*National Centre for Nuclear Research, Pasteura 7, 02-093 Warsaw, Poland*

(Received 5 August 2023; revised 17 October 2023; accepted 31 October 2023; published 14 December 2023)

We performed a search for three-quasiparticle high-K isomer candidates in odd-even Md–Rg nuclei by considering the lowest lying $1\pi 2\nu$ and 3π excitations. Our approach involves calculating the energies of different nuclear configurations using a microscopic-macroscopic model with the Woods-Saxon potential. We explore three pairing scenarios: blocking, quasiparticle method, and particle number projection formalism. The optimal deformations for both ground states and high-K configurations are determined through a four-dimensional energy minimization process. By analyzing the obtained excitation energies, we discuss the most promising candidates for high-K isomers and compare them, where possible, with existing experimental data. We also discuss a possible isomer α-decay hindrance by using calculated Q_α hindrances.

DOI: 10.1103/PhysRevC.108.064309

I. INTRODUCTION

Isomeric states in the domain of superheavy (SH) nuclei are of a considerable interest. Finding them experimentally not only provides clues to a scheme of low-lying single-particle (s.p.) orbits at large Z and N which could be checked against theoretical models but also offers a chance of coming upon longer-lived states of SH isotopes which would then provide new opportunities for their study—see [1–4]. In the present work, we give candidates for the three-quasiparticle (3-q.p.) high-K[1] isomers in odd-even Md–Rg nuclei, which follow from the Woods-Saxon microscopic-macroscopic (MM) model extensively studied in the region of heavy and SH nuclei.

The enhanced stability, or half-life, of some multi-quasiparticle states with high angular momentum and K quantum numbers, situated at relatively low excitation energies, has been investigated a lot in the medium-mass and deformed nuclei [6,7]. It predominantly results from the retardation of electromagnetic transitions—γ rays or internal conversion electrons,[2] connecting states with a sizable difference in K and the absence of typical de-excitation modes with $\Delta K \approx 0$. Both circumstances come into play for a particular placement of a high-K configuration in the nuclear level scheme, when all states below it have significantly smaller K.

A recent progress in experimental studies on excited states in even-even superheavy nuclei, including isomeric ones, allowed for some checks of theoretical models utilized in this region. While the calculated and measured excitation energies can be easily compared, the assignment of particular configurations to the discovered isomeric states often poses substantial difficulties. Typically, the assignments suggested in the literature are based on theoretical models, a knowledge of states in neighboring nuclei, and the systematic patterns observed.

Already 50 years ago, the initial observation of the 0.28 s isomer in ^{254}No was conducted [8]; its isomeric character was confirmed and attributed to the two-quasiproton $K^\pi = 8^-$ configuration in [9]. Its measured energy, 1293 [9,10], 1296 [9], 1295(2) [11], and 1297(2) [12] keV can be compared to values in the range $\langle 1.1\text{–}1.5\rangle$ MeV, obtained in various MM approaches (see Table III in [13]). The experimentally measured excitation energy of the $T_{1/2} = 109(6)$ ms isomer in ^{252}No is approximately 1.25 MeV, as reported in [14,15]. Recently, Kallunkathariyil *et al.* investigated the stability of the 35 µs isomer in the neighboring ^{250}No [16]. In the previous study by Peterson *et al.* [17], its tentative assignment was suggested as two-quasineutron $K^\pi = 6^+$, $\nu 5/2^+[622] \otimes \nu 7/2^+[624]$ configuration. However, its experimental energy is currently unknown. Finally, in a quite recent measurement on the Fragment Mass Analyzer at Argonne National Laboratory, two isomers, 247 and 4.7 µs, were identified in ^{254}Rf. David *et al.* suggested that the shorter-lived one corresponds to a two-quasiparticle configuration, either $\nu^2 8^- = \{\nu 9/2^-[734] \otimes \nu 7/2^+[624]\}$ or $\pi^2 8^- = \{\pi 7/2^-[514] \otimes \pi 9/2^+[624]\}$, while the other one to the 4-quasiparticle configuration $\pi^2 8^- \otimes \nu^2 8^-$ [18].

Concerning experimental studies on odd-even nuclei, a 1.4(1) ms isomer in ^{255}Lr was discovered by using tunnel detectors of the GABRIELA facility [19]. By analyzing the coincidences between isomeric conversion electrons (ICEs) and γ rays, the lower limit of 720 keV was established for the isomer excitation energy. Subsequently, this isomer was also observed at GSI and Berkeley Labs [20,21]. Recently, two isomers, 2.8 ms at an excitation energy $\geqslant 910$ keV in ^{249}Md, and

*michal.kowal@ncbj.gov.pl

[1]The value in question, typically denoted as a K quantum number by the Nilsson notations [5], represents the sum of the total spin projections of the individual single-particle orbitals involved.

[2]Fission probabilities for such nuclei are exceedingly low not only at their ground states but also at their excited states, even up to several MeV, where the majority of high-K states are found.

1.4 ms at $\geqslant 844$ keV in ^{251}Md were reported in [22], following the previous work on spectroscopy in both isotopes [23–25]. As discussed in [3], the configuration assignments for these Lr and Md isomers may be still considered controversial and related to the nature of the $K^{\pi} = 8^{-}$ state in ^{254}No. While its two-neutron configuration is favoured by most interpretations, only a measurement of the splitting of its hyperfine structure can determine whether the state is based on a two-quasiproton or two-quasineutron excitation or a mixture of both (in spite of the very different intrinsic g_K factors: $g_K \approx 1$ for the $\pi 7/2^{-}[514]$ and $\pi 9/2^{+}[624]$ 2q.p. state, and $g_K \approx -0.28$ for $\nu 7/2^{+}[613]$ and $\nu 9/2^{-}[734]$, $|g_K - g_R|$ controlling the intraband decays should be similar, with the rotational g factor $0.7Z/A \leqslant g_R \leqslant Z/A$—see discussion in [3]). The analysis of experimental α-decay data of ^{257}Db and its daughter products led to the conclusion that isomeric states undergoing α-decay exist in ^{257}Db and ^{253}Lr [26].

The most up-to-date information regarding isomers in the heaviest nuclei can be found in the following references: Ackermann *et al.* (2015), Asai *et al.* (2015), Theisen *et al.* (2015), Dracoulis *et al.* (2016), Walker *et al.* (2020), and A. Lopez-Martens with K. Hauschild (2022) [3,13,24,27–29].

A precise prediction of the high-K isomer would require reliable estimates not only of energies but also of EM transition probabilities among various nuclear states and that is beyond the reach of the present theory of heavy nuclei. Instead, one usually finds high-K "optimal" (i.e., obtained by the tilted Fermi surface method) configurations (or close to them) and selects those with low enough energies. For a theoretical overview based on the Nilsson-Strutinsky approach, see the work by Walker *et al.* (2016) [7]. Both experimental studies and theoretical predictions agree that K isomers occur in nuclei near nobelium, rutherfordium, and heavier. The likelihood of K-isomer existence can be attributed to the proximity of high-Ω orbitals to the Fermi level and the predicted deformed subshell gaps around $Z = 100$ and $N = 152$ [30].

In the present work we studied nuclei in the following range of neutron numbers: $N = 142$–166 for Md, Lr, Db, $N = 144$–166 for Bh, $N = 146$–166 for Mt, and $N = 148$–166 for Rg. Compared to studies of K isomers in even-even nuclei like those in [31], the present one (odd-even systems) has to face a significantly larger number of potential candidates. In order to appreciate the uncertainty of the strength of pairing correlations, we study three pairing versions giving different excitation energies of 3-q.p. configurations. We also add some considerations regarding a possible decay of the candidate for isomer to the rotational band built on the one-proton configuration that is included in it. A brief discussion of a possible hindrance of the α decay of high-K configurations is included and illustrated in the extreme case of the predicted Q_α hindrance.

The calculations and selection of candidates for high-K isomers are described in Sec. II, results are presented and discussed in Sec. III, and conclusions are given in Sec. IV. Tables with calculated characteristics of the lowest high-K configurations are provided in the Supplemental Material [32].

II. THE METHOD

Realistic MM or mean-field models predict that Md–Rg nuclei are well deformed in their ground states with axially and reflection-symmetric shapes. This is consistent with the experimentally established characteristics of the rotational bands in the No–Rf region [33–36]. Similar shapes are predicted for excited few-q.p. configurations (as long as no time-reversal-breaking components are included in the mean field), and again, the discovered 2-q.p. K isomers in Fm–Rf nuclei with prominent reduced hindrance factors support this hypothesis. Therefore we assume that the intrinsic parity of considered states is well defined as is their K quantum number.

In order to obtain ground states and configuration-constrained minima, we use a four-dimensional space of deformations $\beta_{\lambda 0}$ defining the nuclear surface:

$$R(\theta) = c(\beta) R_0 \left[1 + \sum_{\lambda=2,4,6,8} \beta_{\lambda 0} \mathrm{Y}_{\lambda 0}(\theta) \right], \qquad (1)$$

where $\mathrm{Y}_{\lambda 0}(\theta)$ are spherical harmonics, $c(\beta)$ is the volume-fixing factor depending on deformation, and R_0 is the radius of a spherical nucleus.

The MM method we use employs the deformed Woods-Saxon (WS) potential [37] and the macroscopic Yukawa-plus-exponential energy model [38] with parameters specified in [39]. In particular, the used pairing strengths are $G_p = (g_{0p} + g_{1p} I)/A$; $G_n = (g_{0n} + g_{1n} I)/A$; $g_{0p} = 13.40$ MeV; $g_{1p} = 44.89$ MeV; $g_{0n} = 17.67$ MeV; $g_{1n} = -13.11$ MeV.

Parameters of the MM model are kept the same as in all recent applications to heavy and superheavy nuclei which concerned masses and deformations [40], Q_α energies [41], the first and second fission barriers in actinides [42], and SH nuclei [43,44]. In the context of many-q.p. excitations, the important feature of the present model is the distinct subshell gap in the neutron spectrum at $N = 152$ around fermium and nobelium, which seems necessary for realistic predictions of K-isomeric states. Two other subshell gaps predicted by the model: at $N = 162$ for neutrons and at $Z = 108$ for protons, not quite confirmed experimentally yet, strongly influence the predictions presented here. The very similar Woods-Saxon model was used in [45,46] which can be consulted for predictions concerning 1-q.p. proton excitations in this region of nuclei.

The MM method used in this study enables the examination of deformation parameters of higher orders. In their work [47,48], Patyk and Sobiczewski observed a wider shell gap around $Z = 100$ and $N = 150$ when incorporating β_{60} in their definition of the nuclear radius. This modification resulted in an improved agreement with existing experimental data. Recently, Liu *et al.* discussed the influence of the deformation parameter β_{60} on the properties of high-K isomers in superheavy nuclei [49]. The shape parametrization used in the present paper includes still one additional parameter, namely, β_{80}.

Ground-state and excited configuration energies are found by the four-dimensional energy minimization over $\beta_{20}, \beta_{40}, \beta_{60}, \beta_{80}$ Eq. (1) performed using the gradient method. To avoid secondary or very deformed minima the minimization is repeated at least 10 times for each configuration with different starting values of deformations.

The pairing is accounted for by using three procedures: 1) the blocking method in which, after removing selected singly occupied states from the set of doubly occupied orbitals, the BCS energy is calculated on the remaining ones at each step of the procedure of minimization over deformations, 2) a more straightforward quasiparticle method in which the BCS q.p. energies for blocked nucleons are added to the energy of the even-even core, and the sum is subjected to the minimization over deformation procedure, and 3) the particle-number-projection (PNP) method in which the energy of the particle-number-projected BCS configuration is minimized over deformations. A short description of the latter procedure is provided in the Appendix. The reason for including various pairing calculations is a deficiency of the BCS method with blocking, used in our mass model for ground state (g.s.) properties of odd-A and odd-odd nuclei when applied to many-q.p. excitations. Usually, the blocking method underestimates excitation energies and pair correlations in many-q.p. states if one uses the pairing strength adjusted to the ground states.

In 2), the microscopic part of the energy for a $1\pi 2\nu$ configuration was taken as the sum of BCS quasiparticle energies of singly occupied levels:

$$E^*_{q.p.} = \sqrt{(\epsilon_\pi - \lambda_\pi)^2 + \Delta_\pi^2} + \sqrt{(\epsilon_{\nu_1} - \lambda_\nu)^2 + \Delta_\nu^2} + \sqrt{(\epsilon_{\nu_2} - \lambda_\nu)^2 + \Delta_\nu^2}$$

and the core energy term consisting of the shell and pairing corrections calculated without blocking. For protons, the core term, as well as the pairing gap Δ_π and the Fermi energy λ_π, are calculated for the odd number of particles, but with the double occupation of all levels. This prescription was used before in [46]. It gives results similar to those obtained when calculating the shell and pairing correction for the even system with one particle less. For 3π 3-q.p. excitations, the microscopic energy was the sum of three proton-quasiparticle energies and the shell and pairing corrections calculated without blocking; as for the $1\pi 2\nu$ excitations, the odd particle number and double occupation of levels were used in the BCS procedure for protons. In the quasiparticle method we use the same pairing strengths as in our mass model. One can mention that the quasiparticle method underestimates 3-q.p. excitation energies at particle numbers for which BCS energy gap vanishes or is very small. Admittedly, it is cruder for 3π than for $1\pi 2\nu$ configurations due to the larger number of blocked quasiprotons.

When using method 3) we face the necessity of adjusting the pairing strengths for neutrons and protons to the new PNP procedure. Within the BCS method, such adjustment can be performed using experimental masses or moments of inertia, like, for example, in [50]. However, with PNP this becomes quite cumbersome. Therefore, we fixed the new strengths $G_n(N,Z)$ for neutrons by so fixing the ratio $G_n(N,Z)/G_n^{\rm mod}(N,Z)$, with $G_n^{\rm mod}(N,Z)$ the strength from our MM model, as to obtain the energy of the 2-q.p. excitations involving two nearly degenerate s.p. levels: the last occupied and the first empty one, close to $2\Delta_n$(BCS) of this model. This corresponds to an increase in pairing strengths by ≈10%. We decided to scale proton pairing strengths by the same factor 1.1 to preserve the original G_p/G_n ratio of the MM model. Such stronger pairing produces smaller nuclear masses (i.e., increases binding) by 3.5–4.5 MeV for studied nuclei. One could try to compensate for this change by subtracting an increased average pairing energy term, but we did not attempt any modification of our mass model. The sole aim of using PNP was to obtain a more realistic estimate for energies of 3-q.p. excitations.

Equilibrium deformations were found by both the blocked BCS and quasiparticle methods for more than 2500 one-proton and two-neutron ($1\pi 2\nu$) and for more than 500 three-proton (3π) 3-q.p. configurations built from s.p. states not too distant from the Fermi surfaces in studied nuclei. The PNP calculations were confined to some selected low-lying 3-q.p. states. Configurations at the lowest excitation energies $E^*_{3\text{-q.p.}}(K)$ are considered as likely candidates for K isomers. We did not consider shifts due to the spin interaction (counterpart of Gallagher shifts for 2q.p.), which for 3-q.p. configurations are not well studied [51,52].

Since a 3-q.p. configuration in an odd-Z deformed nucleus may be thought of as a two-neutron (or a two-proton) excitation built on its one-proton component which is a band head of some rotational band, the probability of de-excitation to this band is one of the factors determining the isomerism. For a $1\pi 2\nu$ configuration with $K = \Omega_\pi + \Omega_{\nu 1} + \Omega_{\nu 2}$, its excitation energy over the one-proton band head with $K_\pi = \Omega_\pi$, $E^*_{3\text{-q.p.}}(K) - E^*_{1q.p.}(\Omega_\pi)$, should be compared to the collective rotational energy: $E^{\rm rot}(I = K, \Omega_\pi) = \frac{1}{2}[K(K+1) - \Omega_\pi^2]/\mathcal{J} = \frac{1}{2}[K_\nu(K_\nu + 2\Omega_\pi + 1) + \Omega_\pi]/\mathcal{J}$, with $K_\nu = \Omega_{\nu 1} + \Omega_{\nu 2}$, and $\mathcal{J}$ is the average moment of inertia of the one-proton q.p. rotational band. For 3π configurations with $K = \sum_1^3 \Omega_{\pi i}$ similar comparisons could be made. The value $(E^*_{3\text{-q.p.}}(K) - E^*_{1q.p.}(\Omega_\pi)) - E^{\rm rot}(I = K, \Omega_\pi)$ gives some indication of a likelihood of the 3-q.p. configuration being isomeric: the smaller it is the less probable is the high-K state de-excitation to the one-proton q.p. rotational band.

Unfortunately, the above energy difference is not a precise indicator of the K isomerism. A customary indicator, the reduced hindrance f_ν, is based on the knowledge of the EM transition depopulating the high-K configuration and its final state: $f_\nu = F^{1/\nu}$, where $F = \tau^\gamma/\tau^W$ is the ratio of the partial EM half-life to its s.p. Weisskopf estimate, $\nu = \Delta K - \lambda$, with ΔK the difference between the initial and final state K values, and λ is the transition multipolarity. As can be seen from the experimental data [6,28], the high-K isomers in deformed nuclei can occur at substantial excitation energies above the yrast line. For example, 2q.p. $K^\pi = 8^-$ isomers in even-even nuclei from various deformed regions, shown in Fig. 12 in [6], which occur 0.5–1.0 MeV above the yrast line still have substantially hindered decays with f_ν values above 30 (typically, f_ν = 30–200 for isomers). Thus, by analogy, 3-q.p. configurations characterized by the energy

differences $(E^*_{3\text{-q.p.}}(K) - E^*_{1q.p.}(\Omega_\pi)) - E^{\rm rot}(I = K, \Omega_\pi) \lesssim 1$ MeV (which are the counterparts of the excitation energies above the yrast line displayed in [6]) can be considered as candidates for isomers, those with smaller differences being preferable. Notice that the rotational energy of levels of a 1q.p. band grows with increasing Ω_π. For example, with $2\mathcal{J} = 170\ \hbar^2$/MeV, the rotational energy at angular momentum $\Omega_\pi + I_R$ with $I_R = 6$ and 11 amounts to 285 and 670 keV, respectively, for $\Omega_\pi = 1/2$, and to 850 and 1530 keV for $\Omega_\pi = 11/2$. Hence, with $\mathcal{J}$ being similar for various one-proton rotational bands, a 3-q.p. configuration containing the lowest proton (i.e., g.s.) orbital with a larger Ω_π has a greater chance to be isomeric.

To estimate rotational energies in studied isotopes we used the calculated cranking moments of inertia of even-even nuclei from [53]. For odd-Z nuclei, we took the average from calculated moments of inertia in neighboring even-even nuclei and increased it by a factor accounting for two effects: overall larger moments of inertia in odd-A vs even-even nuclei as seen in actinides, and the observed increase in $\mathcal{J}$ with rotational frequency (or collective angular momentum) above the cranking value for spin-zero which was given in [53]. For our estimates, we arbitrarily used the factor 1.4. Clearly, an increase in the moment of inertia of the g.s. rotational band makes 3-q.p. high-K configurations more excited with respect to it.

III. RESULTS AND DISCUSSION

Calculated g.s. deformations in considered nuclei change according to the following pattern. The deformations β_{20} are mostly between 0.20 and 0.25, with the largest values for $N = 148$–158, slightly decreasing for $N \geqslant 160$ and with increasing Z. The deformations β_{40} decrease with N by $\approx$0.10 from positive to negative values, starting from $\beta_{40} \approx 0.06$ for $Z = 101, N = 142$, and from $\beta_{40} \approx 0.02$ for $Z = 111, N = 148$. The deformations β_{60} are mostly negative with the largest magnitude for $N = 150, 152$: $\beta_{60} \approx -0.06$ for $Z = 101, N = 150$, and $\beta_{60} \approx -0.03$ for $Z = 111, N = 150$. Finally, the deformations β_{80} are generally small, with the largest values $\beta_{80} \approx 0.03$ for $N = 158, 160$. Equilibrium deformations for the majority of 3-q.p. configurations are close to those of the ground states, which in the case of β_{20} means that it falls within the range ± 0.02 around the ground-state value.

The Woods-Saxon single-particle spectra in Lr isotopes at the calculated g.s. deformations are shown in Figs. 1 and 2. The proton s.p. states with large Ω that can form high-K configurations are (from bottom to top): $\pi 7/2^+_3[633]$, $\pi 7/2^-_3[514]$, $\pi 9/2^+_2[624]$, $\pi 9/2^-_2[505]$, $\pi 11/2^+_1[615]$, and $\pi 7/2^-_4[503]$. Single particle states are labeled by Ω^π_n, with n as the number of the state (counted from the lowest one) within the Ω^π block. The provided Nilsson labels serve to make a connection to the traditional scheme; they have no or little sense for lower Ω values due to their mixing in realistic potentials. Nevertheless, due to the widespread use of Nilsson's notation in the works of other authors, we also decided to use it, mostly in figures, alternately with the Ω^π_n one.

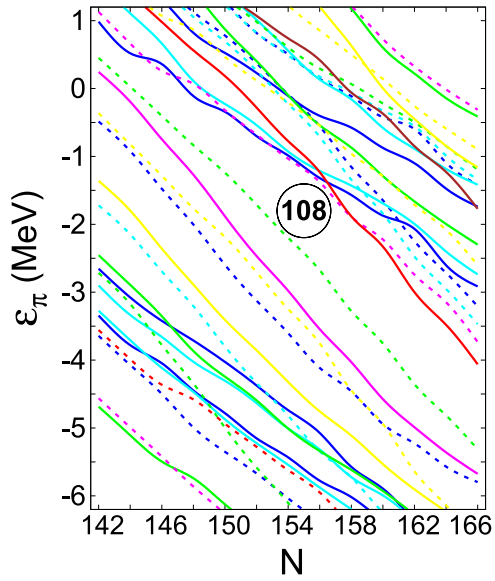

FIG. 1. Single-particle proton levels for Lr isotopes at their equilibrium deformations; negative parity states—dashed, positive parity—solid lines; $\Omega = 1/2$—blue, 3/2—cyan, 5/2—green, 7/2—yellow, 9/2—magenta, 11/2—red, 13/2—brown.

Proton states at the Fermi level in considered odd-Z nuclei determine their g.s. spins and parities. In the quasiparticle scheme, these are in Md: $1/2^-_{10}$ ([521] in the Nilson scheme) with the exception of $7/2^-_3$ for $N = 160$ and $7/2^+_3$ for $N = 166$; in Lr: $7/2^-_3$ except for $9/2^+_2$ for $N = 160, 162, 166$ and $1/2^-_{10}$ for $N = 164$ (for $N = 160$–166 states $9/2^+_2$ and $1/2^-_{10}$ are practically degenerate); in Db: $9/2^+_2$, except for $5/2^-_5$ for $N = 164, 166$; in Bh: $5/2^-_5$; in Mt: $9/2^-_2$ for $N = 146$–152 and $11/2^+_1$ for $N = 154$–166; in Rg: $9/2^-_2$ for $N = 152, 154$,

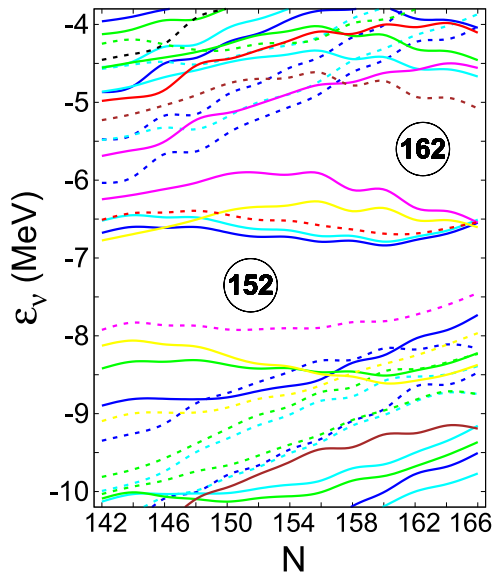

FIG. 2. Single-particle neutron levels for Lr isotopes at their equilibrium deformations; negative parity states—dashed, positive parity—solid lines; $\Omega = 1/2$—blue, 3/2—cyan, 5/2—green, 7/2—yellow, 9/2—magenta, 11/2—red, 13/2—brown, 15/2—black.

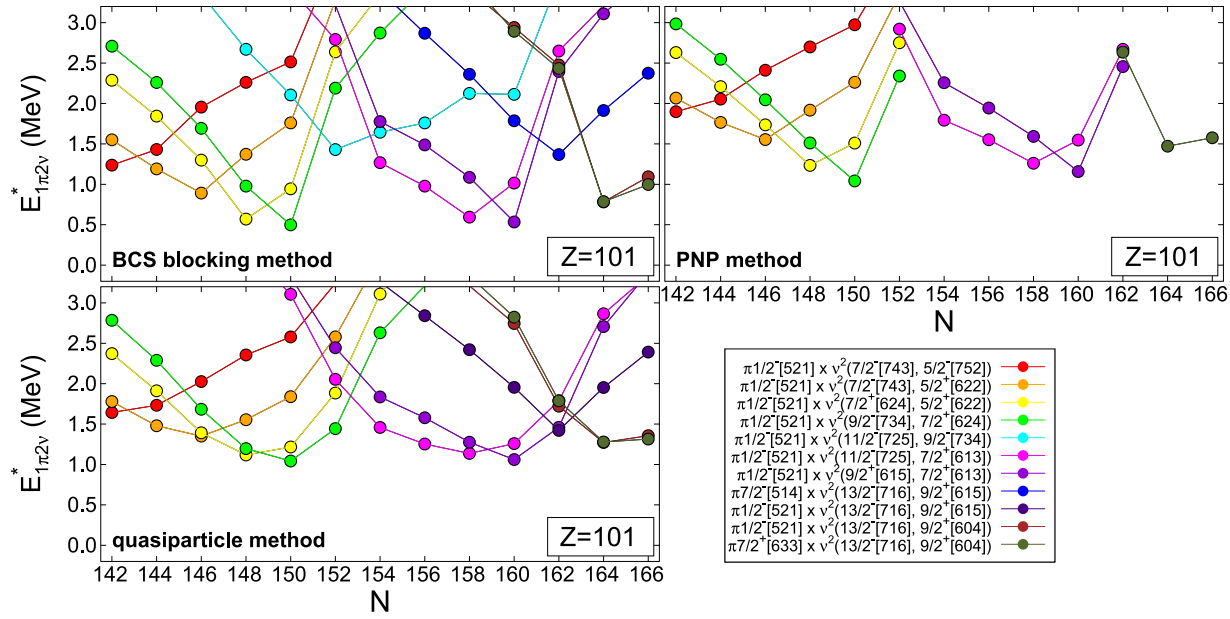

FIG. 3. Calculated excitation energy vs N for $1\pi 2\nu$ large-K configurations which for some N become the lowest in odd-even isotopes of Md; each panel corresponds to the indicated method of calculations.

$3/2^-_8$ for $N = 162$–166 and $11/2^+_1$ for other isotopes, with two high-Ω states being nearly degenerate for $N = 150, 154, 156$. The g.s. spins and parities from the PNP calculation differ from the above only in a few cases.

From a comparison to the experimentally established spins of low-lying states in Md and Lr isotopes around $N = 150$ it follows that the order of proton $\pi 1/2^-_{10}$ and $\pi 7/2^-_3$ states is inverted in the Woods-Saxon potential.

In view of the g.s. deformation changing with Z we have to consider a greater number of two-neutron combinations than necessary for only one isotopic chain. Relevant large - Ω neutron states are (going from bottom to top): $\nu 7/2^-_5[743]$, $\nu 7/2^+_4[624]$, $\nu 9/2^-_3[734]$, $\nu 7/2^+_5[613]$, $\nu 11/2^-_2[725]$, $\nu 9/2^+_3[615]$, $\nu 9/2^+_4[604]$ and $\nu 13/2^-_1[716]$. These states enter the neutron 2-q.p. component of the lowest 3-q.p. configurations in the considered region of nuclei.

A. Excitation energies of $1\pi 2\nu$ 3-q.p. high-K - candidates for isomeric states

From calculated excitation energies of $1\pi 2\nu$ large-K states for six odd-even isotopic chains we select those with the lowest energies at some N. In Fig. 3–8 are shown such candidates and corresponding excitation energies $E^*_{1\pi 2\nu}$ obtained within the standard BCS method with blocking (top left panels), quasiparticle method (bottom left panels), and from the PNP calculation (for selected configurations—top right panels). Tabulated results for five lowest-lying configurations in each isotope obtained in the blocked BCS and quasiparticle method are provided in the Supplemental Material [32].

We rely mostly on pairing calculations within the quasiparticle and PNP schemes, as those with the BCS blocking give too small excitation energies of 3-q.p. configurations. This is expected as BCS solutions with pairing strength adjusted to the g.s. produce too weak correlations or even unpaired solutions when two or three levels are blocked. Results of all three pairing schemes point to the same configurations which we review below. Generally, the isotopic variation of excitation energies is milder within the quasiparticle method than within the PNP and BCS blocking methods.

With a changing neutron number various low-laying two-neutron configurations occur in specific isotopes. One can divide those leading to particularly low-lying high-K states into three groups: type A) in $N = 148$–150 isotopes, type B) in $N = 152$–160 isotopes, and type C) in $N = 164$–166 isotopes. Those energetically favored among others in specific isotopes are: of type A) $\nu^2 6^+\{\nu 7/2^-_5 \otimes \nu 5/2^-_7\}$, $\nu^2 6^-\{\nu 7/2^-_5 \otimes \nu 5/2^+_7\}$, $\nu^2 6^+\{\nu 7/2^+_4 \otimes \nu 5/2^+_7\}$, and $\nu^2 8^-\{\nu 7/2^+_4 \otimes \nu 9/2^-_3\}$; of type B) $\nu^2 9^-\{\nu 7/2^+_5 \otimes \nu 11/2^-_2\}$, $\nu^2 8^+\{\nu 7/2^+_5 \otimes \nu 9/2^+_3\}$, and $\nu^2 10^+\{\nu 9/2^-_3 \otimes \nu 11/2^-_2\}$; of type C) $\nu^2 11^+\{\nu 9/2^-_3 \otimes \nu 13/2^-_1\}$, $\nu^2 11^-\{\nu 9/2^+_4 \otimes \nu 13/2^-_1\}$, and $\nu^2 9^-\{\nu 5/2^+_8 \otimes \nu 13/2^-_1\}$. At the same time, the Woods-Saxon single-neutron level scheme leads to the lowest $1\pi 2\nu$ excitations in $N = 152$ and $N = 162$ isotones lying higher than in the neighboring ones. This effect is weakened by the very small or vanishing BCS neutron gap in the quasiparticle method, but is very prominent with the PNP and the blocked BCS. Below we discuss results for separate isotopic chains, mostly from the quasiparticle scheme. The results of the PNP scheme will be commented on at the end of this subsection.

1. Md

The lowest-lying type-A) configurations are $\pi\nu^2 13/2^-\{\pi 1/2^-_{10} \otimes \nu 7/2^+_4 \otimes \nu 5/2^+_7\}$ (yellow dots in Fig. 3) in ^{249}Md and $\pi\nu^2 17/2^+\{\pi 1/2^-_{10} \otimes \nu 9/2^-_3 \otimes \nu 7/2^+_4\}$ (green dots) in ^{251}Md. The latter, at 1.04 MeV above the g.s., is the lowest-lying type A) state of all. The $\pi\nu^2 15/2^+\{\pi 1/2^-_{10} \otimes \nu 9/2^-_3 \otimes \nu 5/2^+_7\}$ configuration is the second lowest, at similar excitation energy in both isotopes.

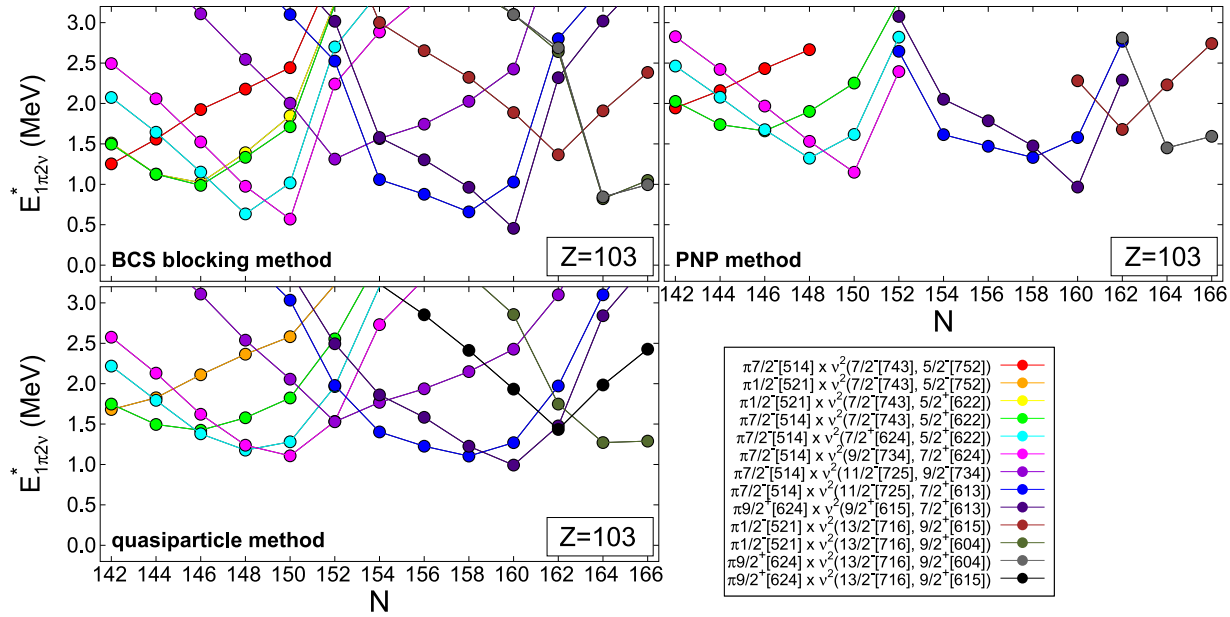

FIG. 4. As in Fig. 3 but for Lr.

Although configurations with $\pi 7/2^-_3$ orbital replacing $\pi 1/2^-_{10}$ lie by 0.25 MeV higher they should be considered in view of the seemingly opposite order of both states in the experiment as compared to the present WS spectrum. In $N = 154, 156, 158$ isotopes the lowest-lying type-B) configuration is $\pi\nu^2 19/2^+\{\pi 1/2^-_{10} \otimes \nu 7/2^+_5 \otimes \nu 11/2^-_2\}$ (magenta dots); $\pi\nu^2 17/2^-\{\pi 1/2^-_{10} \otimes \nu 7/2^+_5 \otimes \nu 9/2^+_3\}$ (dark violets dots) is the lowest one in ^{261}Md; the configurations with $\pi 7/2^-_3$ and $\pi 9/2^+_2$ replacing $\pi 1/2^-_{10}$ are lying 100-200 keV higher, but the first one may be relevant if the proton level order established in $N \approx 150$ isotopes persists in the heavier ones. The type-C) configurations including the two-neutron pair $\{\nu 9/2^+_4 \otimes \nu 13/2^-_1\}$ and one of $\pi 1/2^-_{10}$, $\pi 7/2^+_3$ (dark olive green in Fig. 3) or $\pi 7/2^-_3$, are the favored ones in ^{265}Md (the two first configurations have nearly the same energy), while the ones with the same neutron contents and either $\pi 7/2^+_3$ or $\pi 9/2^+_2$ are the lowest ones in ^{267}Md.

Estimated excitation energies of the lowest $1\pi 2\nu$ configurations above the rotational g.s. structure, discussed in Sec. II, are in $N = 150$ ($K_\nu = 8$): ≈0.6 MeV for $\Omega_\pi = 1/2$ and ≈0.35 MeV for $\Omega_\pi = 7/2$; in $N = 154$ ($K_\nu = 9$): ≈0.95 MeV for $\Omega_\pi = 1/2$ and ≈0.65 for $\Omega_\pi = 7/2$; in $N = 158$ ($K_\nu = 9$): ≈0.55 for $\Omega_\pi = 1/2$ and ≈0.25 for $\Omega_\pi = 7/2$; in $N = 160$ ($K_\nu = 8$): ≈0.6 MeV for $\Omega_\pi = 1/2$ and

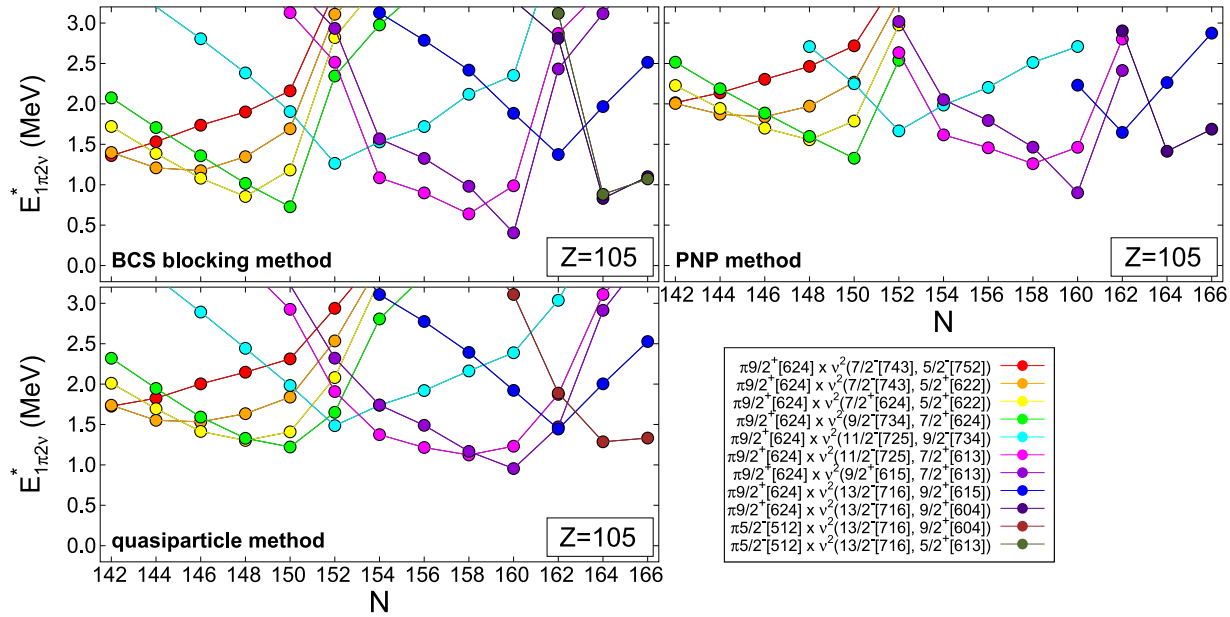

FIG. 5. As in Fig. 3 but for Db.

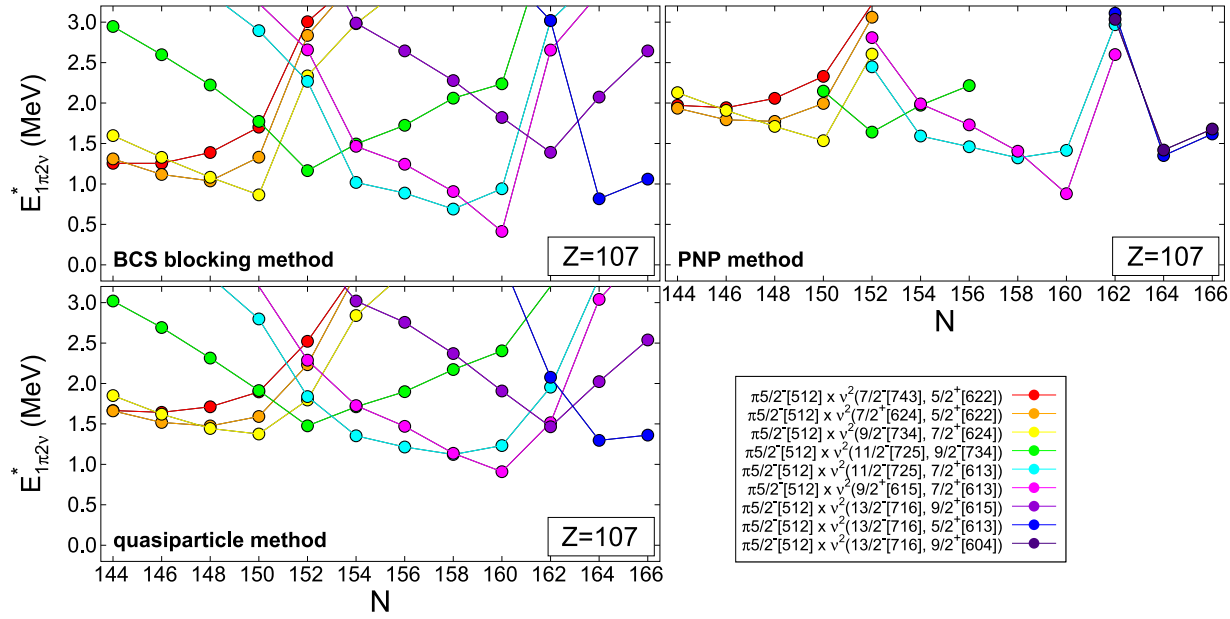

FIG. 6. As in Fig. 3 but for Bh.

≈0.3 MeV for $\Omega_\pi = 7/2$. We have not calculated the moment of inertia for $N = 164$ Md, but assuming that for the Lr isotone one obtains ($K_\nu = 11$): ≈0.45 for $\Omega_\pi = 1/2$ and ≈ −0.25 MeV (the yrast trap) for $\Omega_\pi = 7/2$ (the K mixing of nearly degenerate proton levels would probably remove the trap effect).

2. Lr

The lowest-lying $1\pi 2\nu$ type-A) configurations are $\pi\nu^2 19/2^-\{\pi 7/2^-_3 \otimes \nu 7/2^+_4 \otimes \nu 5/2^+_7\}$ in ^{251}Lr and $\pi\nu^2 23/2^+(25/2^-)\{\pi 7/2^-_3(\pi 9/2^+_2) \otimes \nu 9/2^-_3 \otimes \nu 7/2^+_4\}$ or $\pi\nu^2 21/2^+\{\pi 7/2^-_3 \otimes \nu 9/2^-_3 \otimes \nu 5/2^+_7\}$ in ^{253}Lr (Fig. 4). Configurations with $\pi 1/2^-_{10}$ replacing $\pi 7/2^-_3$ are lying slightly higher. The lowest type B) states are $\pi\nu^2 25/2^+\{\pi 7/2^-_3 \otimes \nu 11/2^-_2 \otimes \nu 7/2^+_5\}$ in ^{261}Lr and $\pi\nu^2 25/2^+\{\pi 9/2^+_2 \otimes \nu 9/2^+_3 \otimes \nu 7/2^+_5\}$ in ^{263}Lr; the configurations with interchanged proton states are predicted as the second lowest in both nuclides. Although not very low-lying, the type C), large-K configurations: $\pi\nu^2 23/2^+\{\pi 1/2^-_{10} \otimes \nu 9/2^+_4 \otimes \nu 13/2^-_1\}$ or $\pi\nu^2 31/2^-\{\pi 9/2^+_2 \otimes \nu 9/2^+_4 \otimes \nu 13/2^-_1\}$ may be good candidates in ^{267,269}Lr.

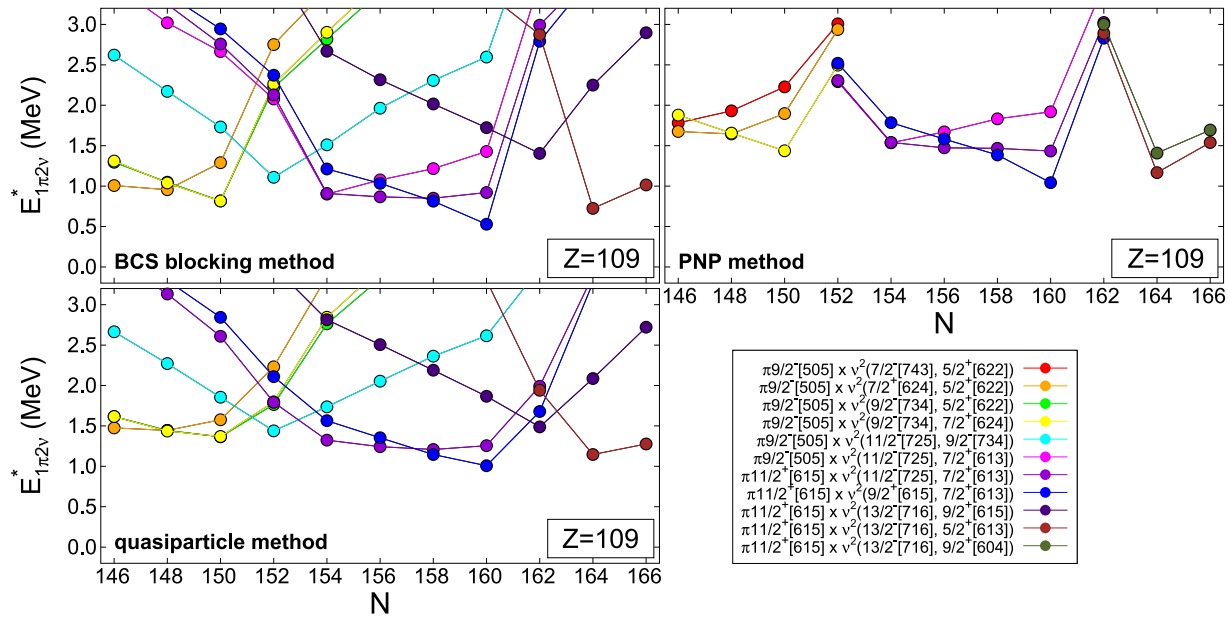

FIG. 7. As in Fig. 3 but for Mt.

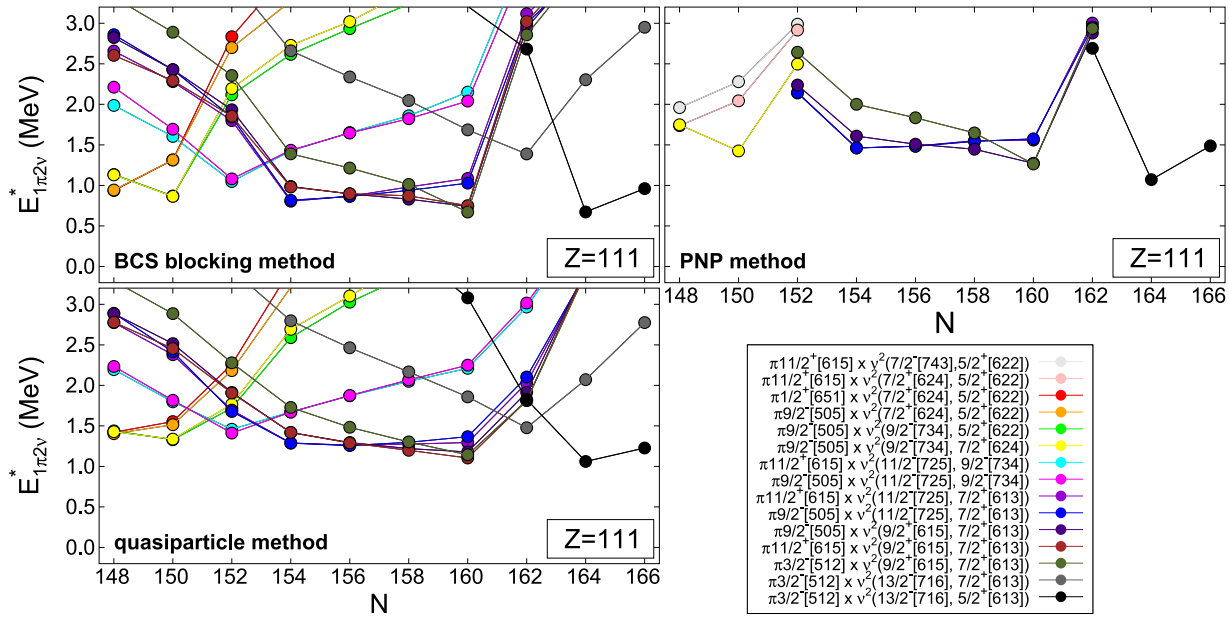

FIG. 8. As in Fig. 3 but for Rg.

3. Db

The most promising candidates occur in the heavier isotopes (type B), $\pi\nu^2 27/2^-\{\pi 9/2^+_2 \otimes \nu 11/2^-_2 \otimes \nu 7/2^+_5\}$, $\pi\nu^2 25/2^+\{7/2^-_3 \otimes \nu 11/2^-_2 \otimes \nu 7/2^+_5\}$ in ^{263}Db and $\pi\nu^2 25/2^+(21/2^-, 23/2^-)\{\pi 9/2^+_2(5/2^-_5, 7/2^-_3) \otimes \nu 9/2^+_3 \otimes \nu 7/2^+_5\}$ in ^{265}Db (Fig. 5). The type A) low-lying configurations are $\pi\nu^2 25/2^-\{\pi 9/2^+_2 \otimes \nu 9/2^-_3 \otimes \nu 7/2^+_4\}$ and $\pi\nu^2 23/2^-\{\pi 9/2^+_2 \otimes \nu 9/2^-_3 \otimes \nu 5/2^+_7\}$ in ^{255}Db, and $\pi\nu^2 21/2^+\{\pi 9/2^+_2 \otimes \nu 5/2^+_7 \otimes \nu 7/2^+_4\}$ in ^{253}Db. Type-C) candidates with sizable K are $\pi\nu^2 31/2^+\{\pi 9/2^+_2 \otimes \nu 13/2^-_1 \otimes \nu 9/2^+_4\}$, $\pi\nu^2 27/2^-\{\pi 5/2^-_5 \otimes \nu 13/2^-_1 \otimes \nu 9/2^+_4\}$ in ^{269}Db and the same neutron pair coupled to $\pi 5/2^-_5$ or $\pi 1/2^-_{10}$ proton states in ^{271}Db. Their estimated excitation above the rotational sequence based on the one-proton component is close to zero for $\Omega_\pi = 5/2$ and even less than zero for $\Omega_\pi = 9/2$. Again, since these states have very similar energies one can expect some K mixing.

4. Bh

The lowest-lying candidate for isomer of all $1\pi 2\nu$ 3-q.p. states is predicted in ^{267}Bh ($N = 160$), in which the configuration $\pi\nu^2 21/2^-\{\pi 5/2^-_5 \otimes \nu 9/2^+_3 \otimes \nu 7/2^+_5\}$ lies at 910 keV (see Fig. 6), at an estimated 0.3 MeV above the rotational g.s. band; the next one, $\pi\nu^2 25/2^+\{\pi 5/2^-_5 \otimes \nu 9/2^+_3 \otimes \nu 11/2^-_2\}$, with K bigger by two units, lies already 300 keV higher. The configuration: $\pi\nu^2 23/2^+\{\pi 5/2^-_5 \otimes \nu 11/2^-_2 \otimes \nu 7/2^+_5\}$ is the lowest in ^{263,265}Bh (this in the $N = 158$ isotone lying 100 keV lower). Type-A) configurations: $\pi\nu^2 21/2^+\{\pi 5/2^-_5 \otimes \nu 9/2^-_3 \otimes \nu 7/2^+_4\}$, $\pi\nu^2 19/2^+\{\pi 5/2^-_5 \otimes \nu 9/2^-_3 \otimes \nu 5/2^+_7\}$ in ^{257}Bh have excitation energy larger by more than 300 keV than the corresponding ones in Md $N = 150$ isotone. Type C) configurations: $\pi\nu^2 23/2^+\{\pi 5/2^-_5 \otimes \nu 13/2^-_1 \otimes \nu 5/2^+_8\}$, $\pi\nu^2 27/2^+\{\pi 5/2^-_5 \otimes \nu 13/2^-_1 \otimes \nu 9/2^+_4\}$ are the most favored in ^{271}Bh ($N = 164$), at estimated 0.7 (0.3) MeV excitation energy above the rotational g.s. band.

5. Mt

Among Mt isotopes the best candidate occurs in ^{269}Mt (type B): $\pi\nu^2 27/2^+\{\pi 11/2^+_1 \otimes \nu 9/2^+_3 \otimes \nu 7/2^+_5\}$, at estimated 0.1 MeV above the rotational g.s. band; the same configuration is the lowest one in ^{267}Mt, but already at the excitation energy by 150 keV higher than in ^{269}Mt (see Fig. 7). The second lowest state in ^{269}Mt: $\pi\nu^2 31/2^-\{\pi 11/2^+_1 \otimes \nu 9/2^+_3 \otimes \nu 11/2^-_2\}$ lies more than 200 keV above the lowest one. Two configurations, $\pi\nu^2 29/2^-\{\pi 11/2^+_1 \otimes \nu 11/2^-_2 \otimes \nu 7/2^+_5\}$, $\pi\nu^2 31/2^-\{\pi 11/2^+_1 \otimes \nu 11/2^-_2 \otimes \nu 9/2^+_3\}$, are the lowest ones in ^{265}Mt. The type-C) candidates in ^{273}Mt are $\pi\nu^2 29/2^-\{\pi 11/2^+_1 \otimes \nu 13/2^-_1 \otimes \nu 5/2^+_8\}$, $\pi\nu^2 33/2^-\{\pi 11/2^+_1 \otimes \nu 13/2^-_1 \otimes \nu 9/2^+_4\}$, the one with lower K lying 200 keV lower. The first one is also the lowest one in the $N = 166$ isotone. Two lowest type-A) configurations are $\pi\nu^2 25/2^+\{\pi 9/2^-_2 \otimes \nu 9/2^-_3 \otimes \nu 7/2^+_5\}$, $\pi\nu^2 23/2^+\{\pi 9/2^-_2 \otimes \nu 9/2^-_3 \otimes \nu 5/2^+_7\}$ in ^{259}Mt.

6. Rg

In this isotopic chain there are many near-degenerate low-lying configurations. The selection shown in Fig. 8 in the left panels corresponds to the lowest in the quasiparticle scheme which may be not lowest in the blocked BCS scheme. The best candidates for isomers occur for $N = 160$ (type-B): $\pi\nu^2 19/2^-\{\pi 3/2^-_8 \otimes \nu 7/2^+_5 \otimes \nu 9/2^+_3\}$, $\pi\nu^2 25/2^-\{\pi 9/2^-_2 \otimes \nu 7/2^+_5 \otimes \nu 9/2^+_3\}$, $\pi\nu^2 27/2^+\{\pi 11/2^+_1 \otimes \nu 7/2^+_5 \otimes \nu 9/2^+_3\}$ in ^{271}Rg and for $N = 164$ (type C): $\pi\nu^2 21/2^+\{\pi 3/2^-_8 \otimes \nu 5/2^+_8 \otimes \nu 13/2^-_1\}$, $\pi\nu^2 19/2^+\{\pi 1/2^-_{11} \otimes \nu 5/2^+_8 \otimes \nu 13/2^-_1\}$, $\pi\nu^2 29/2^-\{\pi 11/2^+_1 \otimes \nu 5/2^+_8 \otimes \nu 13/2^-_1\}$ in ^{275}Rg, see Fig. 8. The C)-type state with $\pi 3/2^-_8$ has the smallest excitation energy of all in Rg isotopes, 1.07 MeV, at an estimated

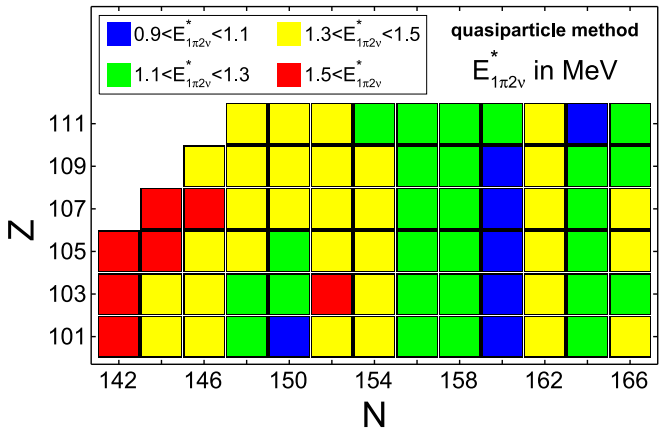

FIG. 9. Map of the lowest $1\pi 2\nu$ 3-q.p. excitation energies calculated with the quasiparticle method.

0.33 MeV above the rotational g.s. band. The excitation energy of the same configuration in the $N = 166$ isotope is ≈200 keV higher. There are less favorable cases in four lighter isotopes: $\pi\nu^2 25/2^+\{\pi 9/2^-_2 \otimes \nu 9/2^-_3 \otimes \nu 7/2^+_4\}$, $\pi\nu^2 17/2^+\{\pi 9/2^-_2 \otimes \nu 9/2^-_3 \otimes \nu 5/2^+_7\}$ in ^{261}Rg, and $\pi\nu^2 29/2^-(27/2^+)\{\pi 11/2^+_1(9/2^-_2) \otimes \nu 11/2^-_2 \otimes \nu 7/2^+_5\}$, $\pi\nu^2 29/2^+(31/2^-)\{\pi 9/2^-_2(11/2^+_1) \otimes \nu 11/2^-_2 \otimes \nu 9/2^+_3\}$, $\pi\nu^2 25/2^-(27/2^+)\{\pi 9/2^-_2(11/2^+_1) \otimes \nu 9/2^+_3 \otimes \nu 7/2^+_5\}$ in ^{265,267,269}Rg.

Figure 9 provides a summary of excitation energies for $1\pi 2\nu$ q.p. configurations from the quasiparticle method. The lowest 3-q.p. energies in each isotope obtained from the PNP calculation are by 0–250 keV larger than from the quasiparticle method (except for $N = 152, 162$ for which the differences are larger), and so are their estimated excitation energies above the rotational g.s. band. Hence, by the energy criterion suggested by data on known K isomers, the PNP calculation also predicts configurations pointed out above as candidates for isomers. In particular, the candidates in $N = 148, 150$ for Md, Lr, Db, and in $N = 158, 160, 164$ isotones seem promising.

B. Excitation energies of three-proton q.p. high-K candidates for isomeric states

There are fewer three-proton q.p. configurations than the $1\pi 2\nu$ ones due to a smaller density of s.p. proton levels and lower Ω values of relevant orbitals. The subshell gap at $Z = 108$ in the deformed WS proton spectrum rises energy of the 3π excitations in Bh ($Z = 107$) isotopes. Even without pairing, their (particle-hole) energies are larger than 1 MeV (or even larger than 1.5 MeV if one excludes the lightest three and the heaviest isotope). The blocked BCS results are unreliable as the proton pairing gap vanishes in 3-.q.p. configurations when one uses pairing strengths of our mass model. All excitation energies obtained from the quasiparticle method are greater than 1.4 MeV, i.e., larger than energies of many $1\pi 2\nu$ states (they are listed in the tables provided in the Supplemental Material [32]). The lowest 3π q.p. excitation energies obtained from the PNP method are smaller than that, in the 0.9–1.0 MeV range, but they occur only for a few

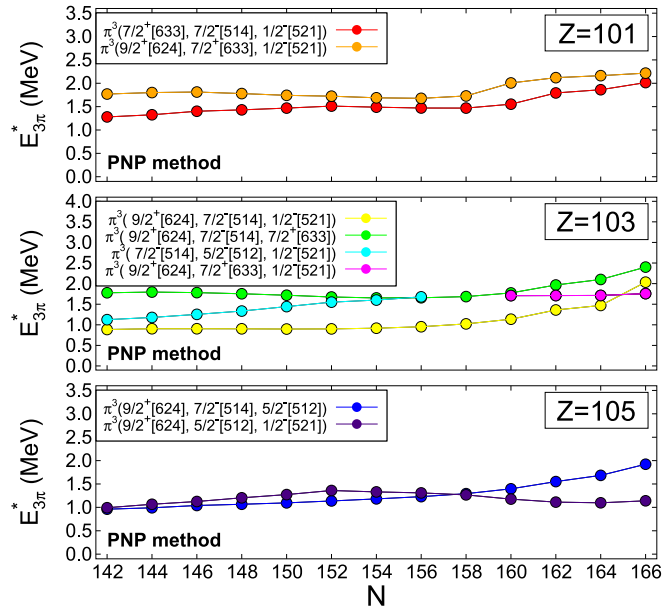

FIG. 10. Excitation energies of low-lying 3π configurations in Md, Lr, and Db with the PNP calculation.

configurations. These smallest PNP energies are smaller than 2Δ(BCS), where the latter is understood as the proton pairing energy gap in the g.s. This might suggest a slightly too small proton pairing strength, but, on the other hand, one may expect a weaker pairing in the 3π q.p. state than in the g.s., so the excitation energies from the quasiparticle method are very likely overestimated.

Energies for favored three-proton q.p. configurations from the PNP and quasiparticle calculations are shown in Figs. 10, 11 and Figs. 12, 13, respectively. In each of these two methods, the lowest 3π states were independently selected. As in the case of $1\pi 2\nu$ states, the obtained excitation energies $E^*_{3\pi}$ depend on the employed pairing version, but the configurations themselves do not. Below, we discuss the results of PNP calculations.

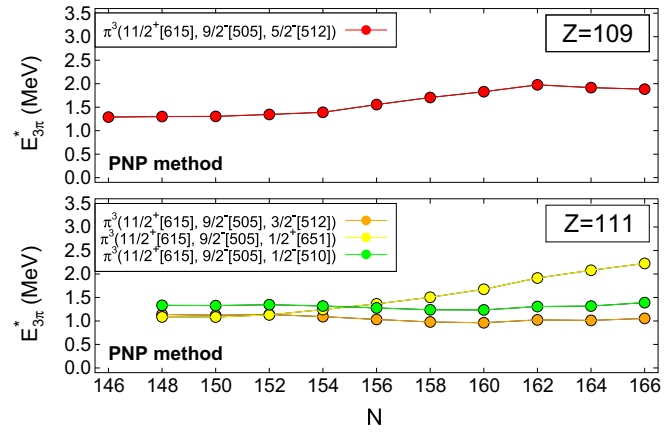

FIG. 11. Excitation energies of low-lying 3π configurations in Mt and Rg with the PNP calculation.

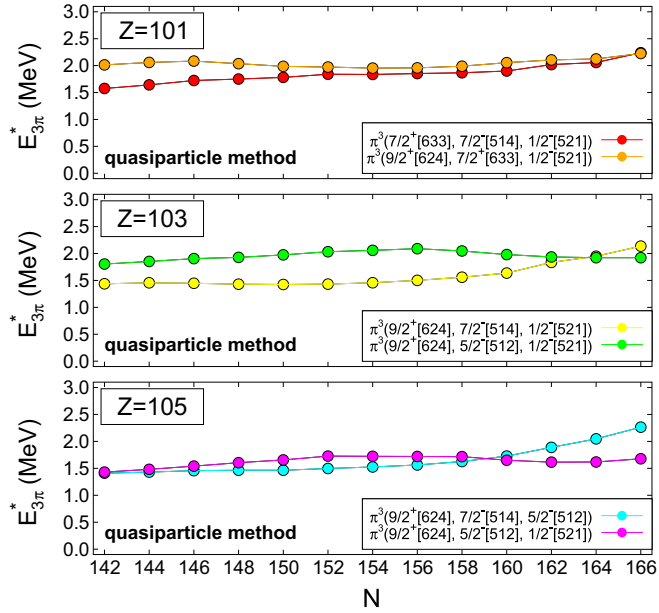

FIG. 12. Excitation energies of low-lying 3π configurations in Md, Lr and Db with the quasiparticle calculation.

1. Md

The lowest 3π q.p. excitation in all studied isotopes is $\pi^3 15/2^+\{\pi 7/2^+_3 \otimes \pi 7/2^-_3 \otimes \pi 1/2^-_{10}\}$, with energy 1.28–1.47 MeV, gently rising from $N = 142$ to $N = 158$; then the rise becomes steeper, with energy reaching 2 MeV at $N = 166$. The second configuration presented in the upper panel in Fig. 10, $\pi^3 17/2^-\{\pi 7/2^+_3 \otimes \pi 9/2^+_2 \otimes \pi 1/2^-_{10}\}$ (orange dots), occurs as the second lowest in isotopes from $N = 150$ to $N = 166$ with energies 1.75–2.2 MeV. In lighter isotopes, two configurations appear below it: $\pi^3 11/2^-\{\pi 7/2^-_3 \otimes \pi 3/2^-_7 \otimes \pi 1/2^-_{10}\}$ and in $N = 142$ also $\pi^3 19/2^+\{\pi 7/2^+_3 \otimes \pi 7/2^-_3 \otimes \pi 5/2^-_5\}$.

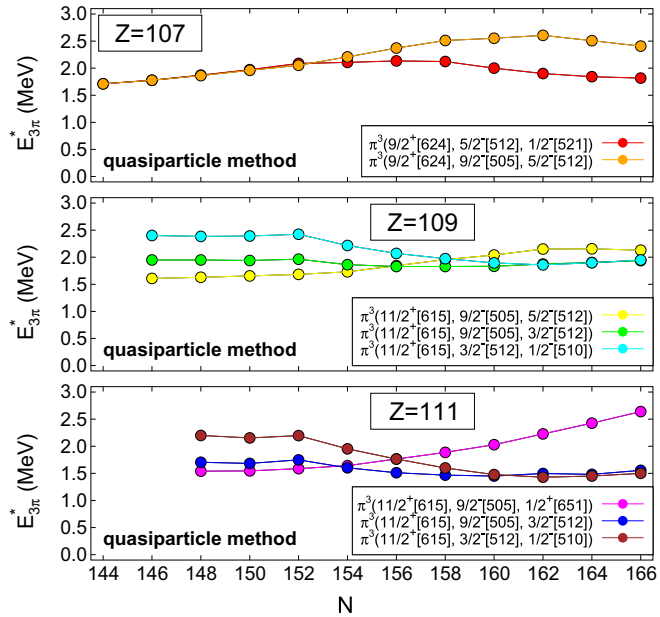

FIG. 13. Excitation energies of low-lying 3π configurations in Bh, Mt, and Rg with the quasiparticle calculation.

2. Lr

The configuration $\pi^3 17/2^+\{\pi 7/2^-_3 \otimes \pi 9/2^+_2 \otimes \pi 1/2^-_{10}\}$ (yellow dots in Fig. 10) is the lowest one in almost all considered isotopes (the only exception is $N = 166$). Its excitation energy stays nearly constant at 0.9–1.0 MeV between $N = 142$ and $N = 158$; then it rises to 2 MeV at $N = 166$. If one accepts the experimental assignment of $1/2^-$ g.s. for ^{253}Lr ($7/2^-$ is predicted from the WS spectrum), then the PNP energy for the state with additional two protons coupled to $K_{2\pi} = 8$ would translate to ≈0.55 MeV excitation above the g.s. rotational band. The configuration $\pi^3 13/2^-\{\pi 7/2^-_3 \otimes \pi 5/2^-_5 \otimes \pi 1/2^-_{10}\}$ is the second lowest in $N = 142$–154. At $N = 156, 158$ the $\pi^3 23/2^-\{\pi 7/2^+_3 \otimes \pi 7/2^-_3 \otimes \pi 9/2^+_2\}$, configuration becomes the second lowest. The configuration $\pi^3 23/2^-\{\pi 9/2^+_2 \otimes \pi 7/2^+_3 \otimes \pi 1/2^-_{10}\}$ (magenta dots in Fig. 10) is the second lowest for $N = 160$–166.

3. Db

Two configurations shown in Fig. 10 are $\pi^3 21/2^+\{\pi 7/2^-_3 \otimes \pi 9/2^+_2 \otimes \pi 5/2^-_5\}$ and $\pi^3 15/2^+\{\pi 5/2^-_5 \otimes \pi 9/2^+_2 \otimes \pi 1/2^-_{10}\}$. The first one is the lowest one for $N < 160$, the second one for $N = 160$–166. Except for those two and the similar configuration $\pi^3 17/2^+\{\pi 7/2^-_3 \otimes \pi 9/2^+_2 \otimes \pi 1/2^-_{10}\}$ all others have considerably larger excitation energies. Estimates of energy difference from the g.s. rotational band built on the $\pi 9/2^+_2$ state are 0.65 MeV for the first ($K_{2\pi} = 6$), and 0.95 MeV for the second ($K_{2\pi} = 3$) configuration, so the first one seems a better candidate for the K isomer.

4. Mt

In Fig. 11 is shown energy of the configuration $\pi^3 25/2^+\{\pi 11/2^+_1 \otimes \pi 9/2^+_2 \otimes \pi 5/2^-_5\}$ which is the lowest one for $N \leqslant 154$. As energies of all 3π 3-q.p. states rise with N, it is probably the best candidate in lighter Mt isotopes. For the $\pi 11/2^+$ g.s. which follows from the PNP calculation and $K_{2\pi} = 7$, one estimates 0.75 MeV excitation above the rotational g.s. band for this candidate in $N = 156$.

5. Rg

The configuration $\pi^3 23/2^-\{\pi 11/2^+_1 \otimes \pi 9/2^+_2 \otimes \pi 3/2^-_8\}$ (orange dots in Fig. 11), the lowest one for $N = 154$–160, seems to be the most interesting candidate. For the $\pi 9/2^+_2$ g.s. following from PNP calculations, with $K_{2\pi} = 7$, one obtains for $N = 160$, ≈250 keV for estimated excitation above the rotational g.s. band.

The above-mentioned results suggest that low-lying 3π high-K configurations appear in Lr, Db, and Rg isotopes. The smallest energies of 3π configuration occur in Lr. Owing to the s.p. structure, the favored 3-q.p. configuration in Rg has a smaller excitation above the g.s. rotational band than the one in Db. The excitation energies $E^*_{3\pi}$ in the quasiparticle method are considerably higher (Figs. 12, 13), but one should allow a correction for the undiminished g.s. pairing Δ it uses. The 3π

isomers in Mt are uncertain and those in Bh unlikely by the energy gap at $Z = 108$.

Regarding our results vs experimental evidence, the candidates for isomers in ^{249,251}Md seem to be of the $2\nu 1\pi$ type, in agreement with the interpretation given in [22]. Configuration similar to the one in ^{251}Md could be isomeric in ^{253}Lr. On the other hand, a similar two-neutron component of the ^{255}Lr isomer, suggested in [21], is not supported by our calculation as the $2\nu 1\pi$ excitations in the $N = 152$ isotones are disfavored, and the 3π configuration looks more favored, cf. Figs. 10, 12. The same conclusion follows from our results for ^{257}Db.

C. Possible α-decay hindrance of high-K isomers

A usual K isomer is recognized by its prolonged EM half-life T_γ. SH nuclei are radioactive and known odd-even SH isotopes undergo mainly α decay (as their fission is usually hindered, see, e.g., review [54]). Thus, there is half-life T_α(g.s.) for the g.s. and the partial half-lives T_α and T_γ for the isomer. When T_α and T_γ are of distinctively different magnitude, the total half-life of the isomer $T_\alpha T_\gamma/(T_\alpha + T_\gamma)$ equals the smaller of the two in good approximation.

The most interesting situation would be a K isomer living longer than the g.s., which requires: $T_\alpha(\text{g.s.}) < \min(T_\alpha, T_\gamma)$. There are two possibilities: $T_\alpha < T_\gamma$ or $T_\alpha > T_\gamma$. In the first case, isomeric γ decay may be more difficult to observe, while two distinct α half-lives T_α(g.s.) and T_α can be detected with generally different Q_α values. The effective half-life of the g.s. α decay after the isomer γ de-excitation, $T_\gamma + T_\alpha$(g.s.), will be statistically suppressed. In the second case, the α decay of the isomer may be difficult to observe, while two α activities will be detected with half-lives T_α(g.s.) and $T_\gamma + T_\alpha$(g.s.) and common Q_α; coincidences with γ/converted electron detectors can help to infer something about the isomer γ-decay scheme and excitation energy $E^*(K)$. When the three considered half-lives are of the similar order, half-lives of three-α activities, and some γ transitions can be detected. When more isomers are present or multiple Q_α values occur, the experimental analysis may become complex.

As stated in the Introduction, we have no way of predicting T_γ. What can be said about the condition $T_\alpha(\text{g.s.}) < T_\alpha$?

One possibility, discussed in [55], is that the excitation of an isomeric configuration in the α-daughter E_d^* is substantially higher than that of the isomer in the parent nucleus E_p^*. As understood from α-decay systematics, the configuration-changing α decays, between states with different K and/or parity, are usually hindered (see, e.g., [56], p 40). If the configuration-preserving decay is suppressed by a reduced $Q_\alpha = Q_\alpha(\text{g.s.}) - \Delta Q_\alpha$, where $\Delta Q_\alpha = (E_d^* - E_p^*)$—as in the situation above—the decay may proceed to different lower-lying configurations. A detailed balance of the corresponding decay rates—a gain due to a greater Q_α (a smaller Q_α hindrance) vs a loss due to a larger configuration-hindrance—is difficult to evaluate. However, one may look for cases of reduced Q_α value in configuration-preserving isomer decays as indicative of possible enhanced isomer stability. We note that phenomenological formulas giving α half-life T_α as a function of Q_α apparently contain some part of this effect so that, *at the same* Q_α, they predict *less probable* g.s.→ g.s. transitions for odd-A and odd-odd nuclei than for the neighboring even-even ones, see, e.g., [57].

The reported example of an isotope with α-decaying K isomer living longer than the g.s. is ^{270}Ds. The α-decay half-life of the 6 ms isomer, with the proposed spin between 8 and 10, is very likely shorter than its γ-decay half-life—see, e.g., the estimate in [58], but longer than the approximately 0.1 ms half-life of the α-decaying ground state [59,60]. One could suspect that the high-K state with a similar structure exists in the daughter nucleus ^{266}Hs; indeed, there is also evidence for a K-isomeric state in ^{266}Hs [60]. The Q_α-hindrance factor effect on the half-life of the ^{270}Dm isomer was estimated within the MM Woods-Saxon model in [55]. It turns out that its logarithm is three times larger than the experimental value, so the effect seems to exist, but is considerably weaker than the pure Q_α hindrance.

We looked for Q_α hindrance among the lowest-lying $1\pi 2\nu$ high-K configurations in the present calculations. The ΔQ_α for structure-preserving α decays show maxima at $N = 154$ and $N = 164$, as dictated by the subshell gaps in the WS s.p. spectrum and seen in Figs. 3–8. The former is bigger in Md, Lr, the latter in Db–Rg, and especially in Mt isotopes. The ΔQ_α obtained in the BCS with blocking are larger than in the quasiparticle method. The largest ΔQ_α occurs in ^{273}Mt: 3.27 MeV in the blocked BCS, 1.62 MeV in the quasiparticle method, and 2.60 MeV in the PNP. Below, we describe this extreme case using PNP energies for the purpose of illustration.

The Q_α hindrance for the decay preserving the lowest-lying $\pi\nu^2$ configuration in ^{273}Mt, $29/2^-\{\pi 11/2^+_1 \otimes \nu 13/2^-_1 \otimes \nu 5/2^+_8\}$, would imply a prolongation of T_α by ≈ 8 orders of magnitude (roughly, 3 orders per 1 MeV ΔQ_α). However, there are many lower-lying possible final $\pi\nu^2$ configurations in ^{269}Bh; among them one with $\pi 5/2^-_5$ instead of $\pi 11/2^+_1$, $\Delta K = -3$, $\Delta Q_\alpha \approx 1.94$ MeV, and one with $\nu 7/2^+_5$ instead of $\nu 5/2^+_8$, $\Delta K = 1$ and $\Delta Q_\alpha \approx 1.43$ MeV, which differ from the initial state *by only one quasiparticle*. There is also a state $29/2^-\{\pi 9/2^+_2 \otimes \nu 13/2^-_1 \otimes \nu 7/2^+_5\}$, with the same K and parity, differing by two quasiparticles, for which $\Delta Q_\alpha = 1.08$ MeV. The presence of many configurations for which the structural hindrance is (at least partly) canceled by a smaller Q_α hindrance suggests that, if the configuration in ^{273}Mt really turns out to be isomeric, its α-decay hindrance will be smaller than the Q_α hindrance. Nevertheless, as long as the predicted subshell gaps are realistic, and all 3qp high-K configurations in ^{269}Bh lie higher than in ^{273}Mt, cf. Figs. 6,7, some α-decay hindrance of the considered configuration should be expected.

IV. CONCLUSIONS

Considering both $1\pi 2\nu$ and 3π 3-q.p. excitations within the MM Woods-Saxon model we have found the candidates for high-K isomers in odd-even Md–Rg isotopes. Using various treatments of pairing we showed that, although they change calculated excitation energies, the favored configurations remain the same. Thus, the presented results may be

treated as specific to the used MM model and determined primarily by the s.p. spectrum of the WS potential. For the same reason, predicted isomer energies should be understood as approximate.

The characteristic features of the results are the numbers Z and N of isotopes in which the high-K states have the lowest excitation energies and the structure of those favored configurations. Particularly favored neutron numbers for $1\pi 2\nu$ states are $N = 148, 150, 158, 160, 164$; the lowest configurations occur in Md for $N = 150$, in Bh for $N = 160$, and in Rg for $N = 164$. A few low-lying 3π configurations occur in Lr, Db, and Rg isotopes; those in Lr and Rg seem more promising due to an estimated smaller excitation over the g.s. rotational band. Our results are consistent with the interpretation of experimental data for K isomers in $N = 148, 150$ isotones of Md and Lr. On the other hand, they suggest 3π rather than $1\pi 2\nu$ structure in $N = 152$ isotones, as $N = 152, 162$ are disfavored for K isomers owing to neutron subshell gaps, as is $Z = 108$ for protons. Certainly, more experimental data are needed to check theoretical predictions and the related s.p. level scheme.

A possible hindrance of a K-isomer α-decay could make it more long-lived than the g.s. The Q_α hindrance can be a reason for such a situation if the structural hindrance is sufficiently strong. The strongest Q_α hindrance follows from our model for $N = 164$ and for heavier isotopes of Mt, with the maximum ΔQ_α for ^{273}Mt.

Clearly, the predictions presented here, based on the extrapolation only partially rooted in experimentally established facts, should be subjected to experimental tests. We hope that they will appear useful in the ongoing research on superheavy nuclei.

ACKNOWLEDGMENTS

M.K. was co-financed by the International Research Project COPIGAL.

APPENDIX: PARTICLE-NUMBER-PROJECTED BCS CALCULATIONS

We specify here procedures used for calculating energy for a state of the BCS-form projected onto a good particle number (separately for neutrons and protons). For PNP to have an effect in the weak pairing limit, one admits parameters λ and Δ unconstrained by the BCS equations. As the projection method itself is well known, see, e.g., [61], the present account is rather brief.

The squared norm, $\langle\Psi \mid \hat{P}_N \mid \Psi\rangle$, of the $N = 2n$-particle component of the BCS wave function $\mid \Psi\rangle = \prod_{\nu>0}(u_\nu + v_\nu a^\dagger_\nu a^\dagger_{\bar\nu}) \mid vac\rangle$, where $\mid vac\rangle$ is the physical vacuum (no particles) and the label ν enumerates states with positive Ω, is equal to the term by ζ^n in the expression $\prod_{\nu>0}(u_\nu^2 + \zeta v_\nu^2)$, which we call P_n. Denoting P^μ_{n-1} the squared norm of the $(N-2)$-particle component of $\mid \Psi\rangle$ with the *omitted* factor $(u_\mu + v_\mu a^\dagger_\mu a^\dagger_{\bar\mu})$, and $P^{\mu\nu}_{n-1}$ is the squared norm of the $(N-2)$-particle component of $\mid \Psi\rangle$ with the *omitted* factors $(u_\mu + v_\mu a^\dagger_\mu a^\dagger_{\bar\mu})(u_\nu + v_\nu a^\dagger_\nu a^\dagger_{\bar\nu})$, one can write the energy of the

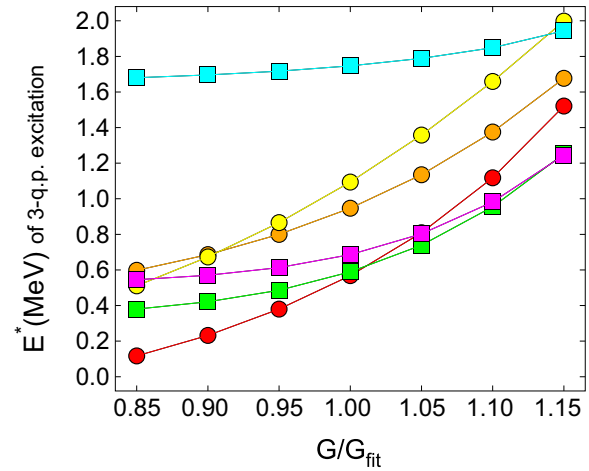

FIG. 14. Energy of the 3-q.p. excitation ($E^*_{1\pi 2\nu}$ or $E^*_{3\pi}$ in MeV) from the PNP method vs pairing strength (in units of the value of the fit $G/G_{\rm fit}$) at the fixed, near g.s. shape, for $1\pi 2\nu$ states in Mt isotopes (dots): $\pi 9/2^-_2 \otimes \nu 7/2^+_4 \otimes \nu 5/2^+_7$ in ^{255}Mt (yellow), $\pi 11/2^+_1 \otimes \nu 9/2^+_3 \otimes \nu 7/2^+_5$ in ^{267}Mt (orange), and ^{269}Mt (red), and for 3π states (squares): $\pi 7/2^-_3 \otimes \pi 9/2^+_2 \otimes \pi 1/2^-_{10}$ in ^{259}Lr (green), $\pi 11/2^+_1 \otimes \pi 9/2^-_2 \otimes \pi 5/2^-_5$ in ^{265}Mt (cyan), and $\pi 9/2^+_2 \otimes \pi 11/2^+_1 \otimes \pi 3/2^-_8$ in ^{271}Rg (magenta).

N-particle projected BCS state as

$$E_N = \frac{\sum_{\mu>0}(2\epsilon_\mu - G)v^2_\mu P^\mu_{n-1} - G\sum_{\mu>0\neq\nu>0} u_\mu v_\mu u_\nu v_\nu P^{\mu\nu}_{n-1}}{P_n}. \tag{A1}$$

The first way to calculate E_N utilizes a representation of ζ as the $(n+1)$-dimensional Jordan block with zero on the diagonal, that means a matrix with elements of the first upper diagonal equal to 1 and all others equal zero. A simple matrix multiplication leads to P_n being the entry $n+1, n+1$ of the matrix $\prod_{\nu>0}(u_\nu^2 + \zeta v_\nu^2)$. After calculating all P^μ_{n-1} in the same way and using the identity $(u^2_\nu v^2_\mu - u^2_\mu v^2_\nu)P^{\mu\nu}_{n-1} = v^2_\mu P^\mu_{n-1} - v^2_\nu P^\nu_{n-1}$, one can calculate Eq. (A1).

In the second method, one uses successive substitutions $\zeta = e^{i\varphi_k}$, with $\varphi_k = 2k\pi/M$, $k = 0, 1,...,M-1$, and sums over k the expressions

$$e^{-in\varphi_k}\prod_{\beta>0}\left(u^2_\beta + e^{i\varphi_k}v^2_\beta\right)\left(\sum_{\mu>0}\frac{(2\epsilon_\mu - G)v^2_\mu e^{i\varphi_k}}{u^2_\mu + e^{i\varphi_k}v^2_\mu} - G\sum_{\mu>0\neq\nu>0}\frac{u_\mu v_\mu u_\nu v_\nu e^{i\varphi_k}}{\left(u^2_\mu + e^{i\varphi_k}v^2_\mu\right)\left(u^2_\nu + e^{i\varphi_k}v^2_\nu\right)}\right). \tag{A2}$$

The formula $\sum_{k=0}^{M-1} e^{i\varphi_k} = (1 - e^{iM\varphi_k})/(1 - e^{i\varphi_k})$ guarantees that so-calculated E_N contains only contributions of $\mid \Psi\rangle$ components with particle numbers $2n$, $2n \pm M$, $2n \pm 2M$, etc. In practical calculations, the value of M like 10 or 15 gives a sufficient accuracy.

We applied both methods described above and checked that they give the same results for E_N.

In order to reduce a search for the optimal projected BCS state to a one-parameter minimization, we eliminate the

dependence of projected energies E_N on λ by imposing the condition for the expected number of particles on each BCS-type function $\Psi(\lambda, \Delta)$: $\langle \Psi_{BCS}(\lambda, \Delta) \mid \hat{N} \mid \Psi_{BCS}(\lambda, \Delta) \rangle = N$, where N is a desired value. The so-obtained energy $E_N(\Delta)$ has a unique minimum as a function of Δ. This minimal value is taken as the energy after projection and minimized over deformations.

The excitation energy of a state with extra two blocked particles relative to the odd-even g.s. includes the effect of deformation change. However, at a fixed deformation, it is a function of the pairing strength G, the neutron one for a $1\pi 2\nu$, and the proton one for a 3π q.p. configuration. This function is shown in Fig. 14 for three $1\pi 2\nu$ and three 3π configurations; the strength G is expressed in units of $G_{\rm fit}$, where $G_{\rm fit}$ is the value from our mass model [41,44] for a given nucleus. The rise in the excitation energy with G is the result of a decrease in energy of both the g.s. and 3-q.p. state, with the former being steeper than the latter.

[1] P. Walker and G. Dracoulis, Nature (London) **399**, 35 (1999).
[2] K. Jadambaa, EPJ Web Conf. **163**, 00030 (2017).
[3] A. Lopez-Martens *et al.*, Eur. Phys. J. A **58**, 134 (2022).
[4] R. D. Herzberg and P. Greenlees, Prog. Part. Nucl. Phys. **61**, 674 (2008).
[5] S. G. Nilsson, Dan. Mat. Fys. Medd. **29**, 1 (1955).
[6] F. G. Kondev *et al.*, At. Data Nucl. Data Tables **103–104**, 50 (2015).
[7] P. M. Walker and F. R. Xu, Phys. Scr. **91**, 013010 (2016).
[8] A. Ghiorso *et al.*, Phys. Rev. C **7**, 2032 (1973).
[9] S. K. Tandel *et al.*, Phys. Rev. Lett. **97**, 082502 (2006).
[10] R.-D. Herzberg *et al.*, Nature (London) **442**, 896 (2006).
[11] F. P. Heßberger *et al.*, Eur. Phys. J. A **43**, 55 (2010).
[12] R. M. Clark *et al.*, Phys. Lett. B **690**, 19 (2010).
[13] C. Theisen *et al.*, Nucl. Phys. A **944**, 333 (2015).
[14] A. P. Robinson *et al.*, Phys. Rev. C **78**, 034308 (2008).
[15] B. Sulignano *et al.*, Phys. Rev. C **86**, 044318 (2012).
[16] J. Kallunkathariyil *et al.*, Phys. Rev. C **101**, 011301(R) (2020).
[17] D. Peterson *et al.*, Phys. Rev. C **74**, 014316 (2006).
[18] H. M. David *et al.*, Phys. Rev. Lett. **115**, 132502 (2015).
[19] K. Hauschild *et al.*, Phys. Rev. C **78**, 021302(R) (2008).
[20] S. Antalic *et al.*, Eur. Phys. J. A **38**, 219 (2008).
[21] H. B. Jeppesen *et al.*, Phys. Rev. C **80**, 034324 (2009).
[22] T. Goigoux *et al.*, Eur. Phys. J. A **57**, 321 (2021).
[23] A. Chatillon *et al.*, Eur. Phys. J. A **30**, 397 (2006).
[24] M. Asai, F. P. Heßberger, and A. Lopez-Martens, Nucl. Phys. A **944**, 308 (2015).
[25] R. Briselet *et al.*, Phys. Rev. C **102**, 014307 (2020).
[26] F. Heßberger *et al.*, Eur. Phys. J. A **12**, 57 (2001).
[27] D. Ackermann, Nucl. Phys. A **944**, 376 (2015).
[28] G. D. Dracoulis, P. M. Walker, and F. G. Kondev, Rep. Prog. Phys. **79**, 076301 (2016).
[29] P. Walker and Z. Podolyák, Phys. Scr. **95**, 044004 (2020).
[30] P. T. Greenlees *et al.*, Phys. Rev. C **78**, 021303(R) (2008).
[31] H. L. Liu, P. M. Walker, and F. R. Xu, Phys. Rev. C **89**, 044304 (2014).
[32] See Supplemental Material at http://link.aps.org/supplemental/10.1103/PhysRevC.108.064309 for tables of five lowest configuration energies, with corresponding deformations, in each isotope obtained for $1\pi 2\nu$ states within the blocking (Table I) and quasiparticle method (Table II), and for 3π states within the quasiparticle method (Table III).
[33] R.-D. Herzberg *et al.*, Phys. Rev. C **65**, 014303 (2001).
[34] S. Ketelhut *et al.*, Phys. Rev. Lett. **102**, 212501 (2009).
[35] S. Eeckhaudt *et al.*, Eur. Phys. J. A **26**, 227 (2005).
[36] P. T. Greenlees *et al.*, Phys. Rev. Lett. **109**, 012501 (2012).
[37] S. Ćwiok, J. Dudek, W. Nazarewicz, J. Skalski, and T. Werner, Comput. Phys. Commun. **46**, 379 (1987).
[38] H. J. Krappe, J. R. Nix, and A. J. Sierk, Phys. Rev. C **20**, 992 (1979).
[39] I. Muntian, Z. Patyk, and A. Sobiczewski, Acta Phys. Pol. B **32**, 691 (2001).
[40] M. Kowal, P. Jachimowicz, and A. Sobiczewski, Phys. Rev. C **82**, 014303 (2010).
[41] P. Jachimowicz, M. Kowal, and J. Skalski, Phys. Rev. C **89**, 024304 (2014).
[42] P. Jachimowicz, M. Kowal, and J. Skalski, Phys. Rev. C **85**, 034305 (2012); **101**, 014311 (2020).
[43] P. Jachimowicz, M. Kowal, and J. Skalski, Phys. Rev. C **95**, 014303 (2017).
[44] P. Jachimowicz, M. Kowal, and J. Skalski, At. Data Nucl. Data Tables **138**, 101393 (2021).
[45] S. Ćwiok and S. Hofmann, Nucl. Phys. A **573**, 356 (1994).
[46] A. Parkhomenko and A. Sobiczewski, Acta Phys. Pol. B **35**, 2447 (2004); **36**, 3115 (2005).
[47] Z. Patyk and A. Sobiczewski, Nucl. Phys. A **533**, 132 (1991).
[48] Z. Patyk and A. Sobiczewski, Phys. Lett. B **256**, 307 (1991).
[49] H. L. Liu, F. R. Xu, P. M. Walker, and C. A. Bertulani, Phys. Rev. C **83**, 011303(R) (2011).
[50] N. Minkov, L. Bonneau, P. Quentin, J. Bartel, H. Molique, and D. Ivanova, Phys. Rev. C **105**, 044329 (2022).
[51] N. I. Pyatov and A. S. Chernyehev, Izv, ANSSR, Seria, Fiz. **28**, 1173 (1964).
[52] K. Jain and A. K. Jain, Phys. Rev. C **45**, 3013 (1992).
[53] A. Sobiczewski, I. Muntian, and Z. Patyk, Phys. Rev. C **63**, 034306 (2001).
[54] F. P. Heßberger, Eur. Phys. J. A **53**, 75 (2017).
[55] P. Jachimowicz, M. Kowal, and J. Skalski, Phys. Rev. C **98**, 014320 (2018).
[56] F. P. Hessberger, arXiv:2102.08793.
[57] G. Royer, Q. Ferrier, and M. Pineau, Nucl. Phys. A **1021**, 122427 (2022).
[58] J. Khuyagbaatar, Eur. Phys. J. A **58**, 243 (2022).
[59] S. Hofmann, F. P. Hessberger *et al.*, Eur. Phys. J. A **10**, 5 (2001).
[60] D. Ackermann *et al.*, GSI Sci. Rep. **2011**, 208 (2012).
[61] P. Ring and P. Schuck, *The Nuclear Many-Body Problem* (Springer-Verlag, New York, 1980).